The Journal of Engineering

The 14th IET International Conference on AC and DC Power Transmission (ACDC 2018)

IET Journals
The Institution of Engineering and Technology

Maximum power point tracking scheme with partial shading detection for two-stage grid-connected photovoltaic inverters

eISSN 2051-3305
Received on 23rd August 2018
Accepted on 19th September 2018
E-First on 15th January 2019
doi: 10.1049/joe.2018.8547
www.ietdl.org

Lei Huang[1,2], Jiyuan Zhang[1,2], Qiong Cui[1], Hao Wang[1], Jie Shu[1,2] ✉

[1]Key Laboratory of Renewable Energy, Guangzhou Institute of Energy Conversion of Energy Conversion, Chinese Academy of Sciences, No. 2, Nengyuan Rd., Wushan, Tianhe District, Guangzhou, People's Republic of China

[2]University of Chinese Academy of Sciences, No.19A Yuquan Road, Shijingshan District, Beijing, People's Republic of China

✉ *E-mail: shujie@ms.giec.ac.cn*

Abstract: This paper proposes a maximum power point tracking (MPPT) method with partial shading (PS) detection based on modified PI incremental conductance (IC) for photovoltaic inverters. To accurately trigger the algorithm, a PS detecting approach based on voltage deviation is derived through the comparison of voltage and current characteristics under uniform and non-uniform insolation. To track the global maximum power point (GMPP) precisely and fast, a global search scheme considering appropriate voltage reference, search direction and termination criteria is presented. The modified PI-based IC method is implemented in the local search process. In order to verify the effectiveness of the algorithm, the proposed method is utilised in the two-stage grid-connected photovoltaic inverters built in MATLAB/Simulink. The performance of the scheme is compared with the traditional IC method under step-changing and gradual-changing insolation and various temperature. In all simulation cases, the proposed approach can identify the PS with multiple local maxima, accurately trigger the global search process and track the GMPP. The search periods are around 0.1–0.2 s, and the efficiencies of PV generation under steady state are normally above 99.5%. The presented method can improve the efficiency of distributed and centralised PV system.

1 Introduction

In a PV system, key factors affecting the system yield include PV module harvest, PV array topology, MPPT method, and conversion efficiency. Among these factors, MPPT is one critical component of any PV system because it is the most economical way to increase the overall PV system productivity [1, 2].

The voltage output of a PV module is normally <100 V and lower than the inverter input requirement in most PV systems. So PV modules must be connected serially to form a higher voltage output. However, because of the non-linear characteristics of *I–V* relation, multiple power peaks appear in the *P–V* curve when the entire PV array connected to the same inverter does not receive homogeneous insolation, which makes the tracking more complicated [3]. The conventional algorithms, such as perturb & observe (P&O) [4–6] and incremental conductance (IC) [7, 8], lack of the ability to track the GMPP. Consequently, it is critical to develop MPPT techniques adaptable for non-uniform insolation.

Over the last decade, a large amount of researches have been reported to address the problem caused by partial shading (PS) effect by new MPPT approaches [9, 10]. These approaches mainly include three groups, namely modified conventional methods [11–14], soft computing based techniques [15–22], and PV array topology-based techniques [23, 24]. The PV array topology-based techniques arouse less interest than the other two. The main reason is the increasing cost of devices and insufficient voltage output for large-scale systems. The other two groups attract immense interest in PV research communities.

One critical process of the modified conventional MPPT methods and soft computing-based GMPP techniques is the initialisation process. This process is used to activate the global search process or the soft computing-based techniques to track the GMPP when the insolation, temperature, and loads change. Common references for the initialisation process include PV voltage, current, and power. According to the carried out researches, there are four main kinds of initialisation processes. The first one is initialisation by PV power variation and time [11, 20, 25], and it cannot distinguish PS and uniform insolation. The second one is initialisation by PV current and time [21, 26], and it cannot distinguish PS and uniform insolation either. The third one is initialisation by PV power and current [27], and it depends on PV array and has a PS detection ability and can distinguish PS and uniform insolation. The fourth one is initialisation by PV voltage and current [12, 28], and it depends on PV array and some can succeed in PS detection [29].

This paper presents a modified PI-IC MPPT scheme with a PS detection process, consisting of a global and local search process for the PV array under PS and uniform isolation. The local search process utilises a variable step size PI-IC method. The global search process employs a more precise variable step size PI-IC method with a PV system-dependent searching scheme. The remainder of this paper is organised as follows. Section 2 provides the model of a PV array, critical observations under PS and the MPPT scheme with PS detection base on modified PI-IC method. Section 3 provides simulation results and discussion to validate the proposed approach under variation of insolation and temperature. Finally, Section 4 concludes the paper.

2 Methodology

2.1 Model of A PV module

For an ideal PV module, the *I–V* relation can be described by the following equation.

$$I_{\mathrm{md}} = I_{\mathrm{ph,md}} - I_{\mathrm{s,md}}\left(\mathrm{e}^{(q(V_{\mathrm{md}}+I_{\mathrm{md}}R_{\mathrm{s,md}}))/nN_skT}-1\right) - \frac{V_{\mathrm{md}}+I_{\mathrm{md}}R_{\mathrm{s,md}}}{R_{\mathrm{sh,md}}} \tag{1}$$

where I_{md} and V_{md} are the terminal current and voltage of the PV module, $I_{\mathrm{ph,md}}$ is the photocurrent, $I_{\mathrm{s,md}}$ is the diode equivalent reverse saturation current, $R_{\mathrm{s,md}}$ is the series resistance, $R_{\mathrm{sh,md}}$ is the shunt resistance, n is the diode equivalent ideality factor, N_s is the number of cells in a module, T is module temperature in Kelvin, k is Boltzmann constant (1.38×10^{-23} J/K), and q is the elementary charge (1.6×10^{-19} C).

In a silicon PV module, solar cells are serially connected. If some solar cells are partially shaded, the output of the module drops according to the shaded cell's current limitation. Therefore,

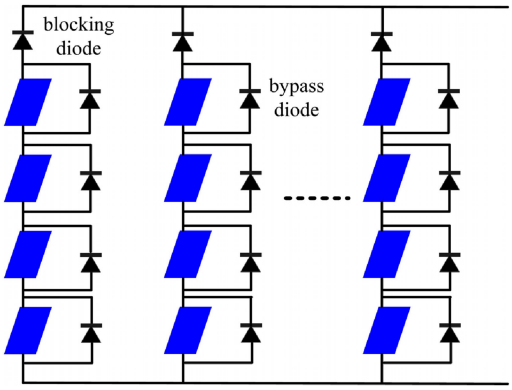

Fig. 1 *Typical structure of a PV array*

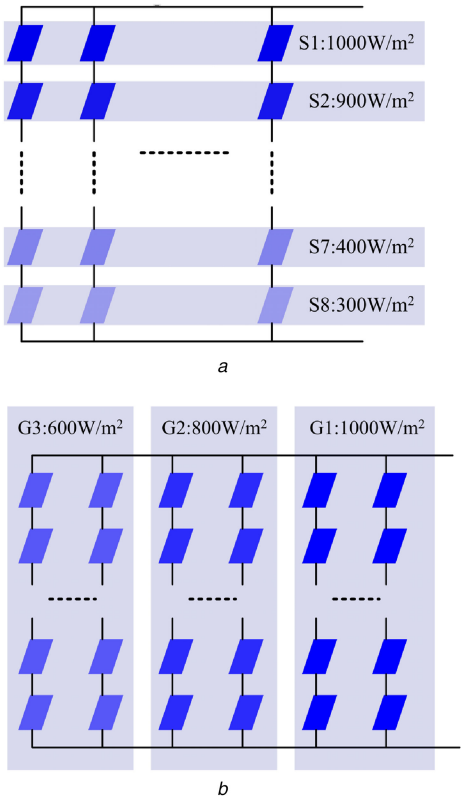

Fig. 2 *Partial shading in a PV array with eight modules in strings*
(a) Non-uniform insolation in strings, ***(b)*** Non-uniform insolation in groups

to eliminate the PS influence, a PV module is integrated two or three bypass diodes, each diode for 18 or 24 solar cells.

2.2 Model of a PV array

Fig. 1 shows a typical structure of a PV array. Classically, PV modules are connected in strings to meet the input requirement of inverters. Furthermore, strings are usually connected in parallel to reduce cost and improve system productivity in high-capacity and high-voltage applications. Due to the parallel construction, the mismatch in output voltage leads to the load pattern of some modules and significant reduction of PV array output power. Therefore, each string is integrated with a blocking diode to prevent reverse current.

As of the PV module characteristic, when the module has non-uniform insolation, multiple maxima of the *P–V* curve appear. For a PV array, the maximum number of local maxima is equal to the number of bypass diodes per string. To better comprehend the effect of non-uniform insolation on a PV array, two kinds of shading are depicted in Fig. 2, and their *P–V* and *I–V* curves are shown in Fig. 3. Each string of this PV array consists of eight modules. In Fig. 2*a*, PV array is divided into eight subassemblies, and each subassembly has uniform insolation, while the modules in same string have different insolation varying from 1000 W/m^2 to 300 W/m^2 with a step size of 100 W/m^2. As shown in Fig. 3, the *P–V* curve under this shading has eight peaks because eight subassemblies have different insolation. In Fig. 2*b*, PV array is divided into three groups, and each group has uniform insolation varying from 1000 W/m^2 to 600 W/m^2 with a step size of 200 W/m^2. As shown in Fig. 3, there is only one peak in the *P–V* curve under this PS condition. The whole array is considered as one subassembly in this condition, and the peak number is equal to the subassembly number. Therefore, not all PS leads to multiple peaks, but only those resulting in non-uniform insolation of strings do.

2.3 Critical observations under partial shading

I–V curve with two peaks is discussed for conducting the detection method of PS. It is assumed that, under this PS condition (condition A), the PV array is divided into two subassemblies with different insolation, 650 W/m^2 (condition A-1) and 1000 W/m^2 (condition A-2). The *I–V* curve is shown in Fig. 4. The voltage of GMPP is around 325 V, and the voltage of the other LMPP is around 450 V. To compare the difference between uniform insolation and PS conditions, it is also assumed a uniform insolation condition producing the same PV current as the PV array under condition A, 685 W/m^2 (condition B). Fig. 5 shows the *I–V* curves of the partial-shading PV modules and the unshaded modules of the same area size under condition A, and the *I–V* curve of the same PV modules of the same area size under uniform insolation of 685 W/m^2 (condition B-1) producing the same operating current value under MPP as condition A. The PV array is working at local MPP under condition A and at GMPP under condition B. The PV array current is the same under these conditions.

The local MPP with the maximum voltage is always the operating point using conventional MPPT schemes. Therefore, this point could be used to discern the insolation levels of a PV array. According to the simulation results, the three operating points in Fig. 5, also the LMPP with maximum voltage, have a voltage relation described as follows:

$$V_{A-1} + V_{A-2} \simeq 2V_{B-1} \tag{2}$$

where $V_{A\text{-}1}$, $V_{A\text{-}2}$, $V_{B\text{-}1}$ are, respectively, the voltages of the same size PV modules at operating point A-1, A-2, and B-1.

To describe the PV array voltage difference between conditions A and B, it is assumed that the array area is A_r of which area A_x is shaded under condition A. The difference is described as follows:

$$V_A - V_B = \left(V_{A-1} + V_{A-2} + \frac{A_r - 2A_x}{A_x} V_{A-2}\right) - \frac{A_r}{A_x} V_{B-1} \tag{3}$$

where V_A, V_B are PV array voltages under conditions A and B, respectively.

The authors substitute (2) into (3) and attain (4):

$$V_A - V_B = -\frac{A_r - 2A_x}{A_x}(V_{A-2} - V_{B-1}) \tag{4}$$

In (4), as the shaded area decreases and the insolation difference increases, the effect of PS becomes more severe, and the difference between V_A and V_B increases. Therefore, the authors could use this difference to detect the PS by setting a voltage threshold. When the PV module is under uniform insolation, PV current and voltage have the following relation:

$$I_{sc,md} = I_{sc,md,STC}\frac{S}{S_{STC}}[1 + \alpha_{sc}(T - T_{STC})] \tag{5}$$

$$I_{sc,md} = I_{sc,md,STC}\left(\frac{T}{T_{STC}}\right)^3 exp\left[\frac{E_g}{k}\left(\frac{1}{T_{STC}} - \frac{1}{T}\right)\right] \tag{6}$$

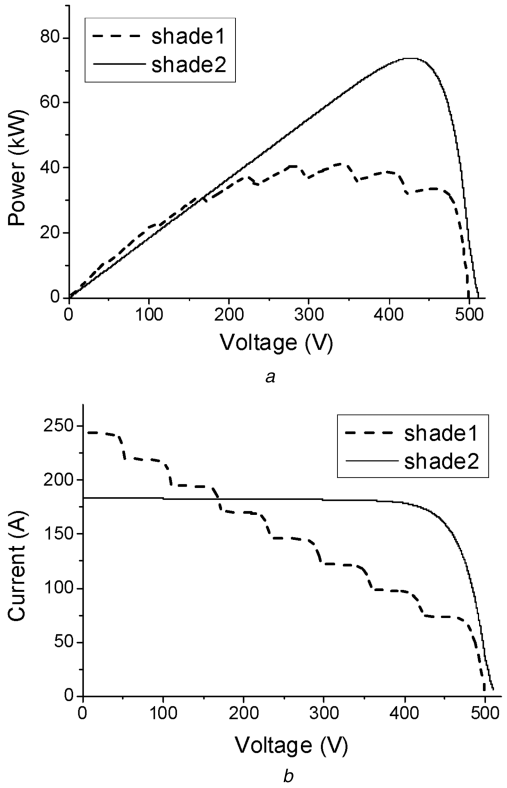

Fig. 3 *PV array characteristics under partial shading*
(a) *P–V* curves, ***(b)*** *I–V* curves

$$I_{s,md,STC} = I_{sc,md,STC} exp\left(-\frac{q}{N_s n_{STC} kT} V_{oc,md,STC}\right) \quad (7)$$

where $I_{sc,md}$ is the PV module short-circuit current, $I_{sc,md,STC}$ is the short-circuit current under STC, S is solar insolation, S_{STC} is the solar insolation under STC, 1000 W/m^2, α_{sc} is temperature coefficient of short-circuit current, T_{STC} is the temperature under STC, 298 K, $I_{s,md}$ is the PV module diode equivalent reverse saturation current, $I_{s,md,STC}$ is PV module diode equivalent reverse saturation current under STC, E_g is energy bandgap, n_{STC} is diode equivalent ideality factor under STC, and $V_{oc,md,STC}$ is PV module open-circuit voltage under STC.

First, the insolation change is only considered. The authors attain (8) by solving (5)–(7):

$$V_{oc,md} = \frac{N_s n_{STC} kT}{q} \ln\frac{I_{sc}}{I_s} = V_{oc,md,STC} + \frac{N_s n_{STC} kT}{q} \ln\frac{S}{S_{STC}} \quad (8)$$

where $V_{oc,md}$ is the PV module open-circuit voltage.

Second, the temperature dependence is added into (8) by adding the open-circuit voltage temperature coefficient β_{oc}. Then, the authors attain (9): (see (9)) . To obtain the PV array MPP voltage V_{mp}, (9) is used to derive V_{mp} as V_{mp} and V_{oc} have a very close temperature coefficient and similar variation law. The formula of V_{mp} could be derived approximately as follows:

$$V_{mp} = N_{ser}[1 + \beta_{oc}(T - T_{STC})] \times \left(V_{mp,md,STC} + \frac{N_s n_{STC} kT}{q} \ln\frac{S}{S_{STC}}\right) \quad (10)$$

where N_{ser} is the number of modules in a PV string, V_{mp} is the PV array MPP voltage, and $V_{mp,md,STC}$ is the MPP voltage of PV module under STC.

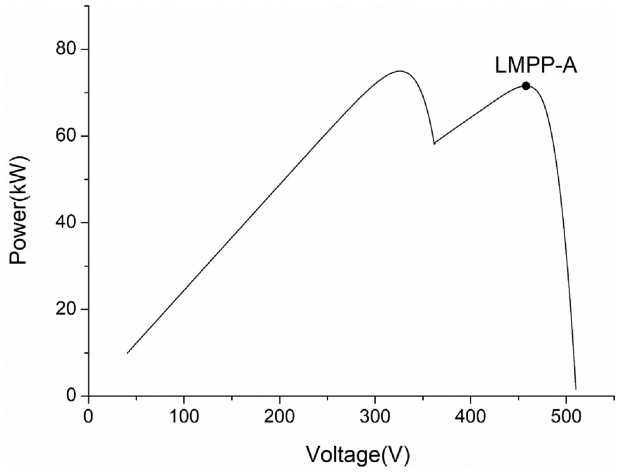

Fig. 4 *P–V curve of PV array with two peaks under partial shading*

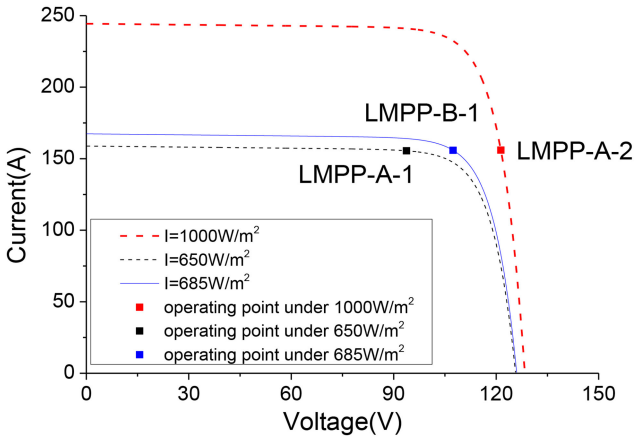

Fig. 5 *I–V curves of modules with the same size under different insolation*

Considering the PV array MPP current I_{mp} largely depends on solar insolation and its correlation with temperature is extremely weak, the authors can use I/I_{mp} to substitute S/S_{STC} in (10). Thus, the MPP voltage of V_B can be calculated as follows:

$$V_{mpc} = N_{ser}[1 + \beta_{oc}(T - 298)] \times \left(V_{mp,md,STC} + \frac{N_s nkT}{q} \ln\frac{I_{mp}}{I_{mp,STC}}\right) \quad (11)$$

where V_{mpc} is the calculated value of V_B, it is an approximation of the calculated maximum voltage.

2.4 MPPT scheme base on modified PI-IC method

The proposed MPPT scheme based on modified PI-IC method has three essential processes, namely global search process, local search processes and initialisation process. The initialisation process is based on the variation of the PV array power and voltage to detect the PS. If PS is detected, the global process is activated to hunt the GMPP by scan scheme through setting reference voltages and using IC method with variable step size. The scan direction, scope and termination criteria of the global process depend on the PV array characteristic. After the GMPP is found, it enters the local process to trace the GMPP precisely with a modified variable step size PI-IC method.

2.4.1 Initialisation process: When the algorithm is under local search process, the initialisation process is started if the insolation changes. The change of the insolation results in the variation of the

$$V_{oc,md} = [1 + \beta_{oc}(T - T_{STC})]\left(V_{oc,md,STC} + \frac{N_s n_{STC} kT}{q} \ln\frac{S}{S_{STC}}\right) \quad (9)$$

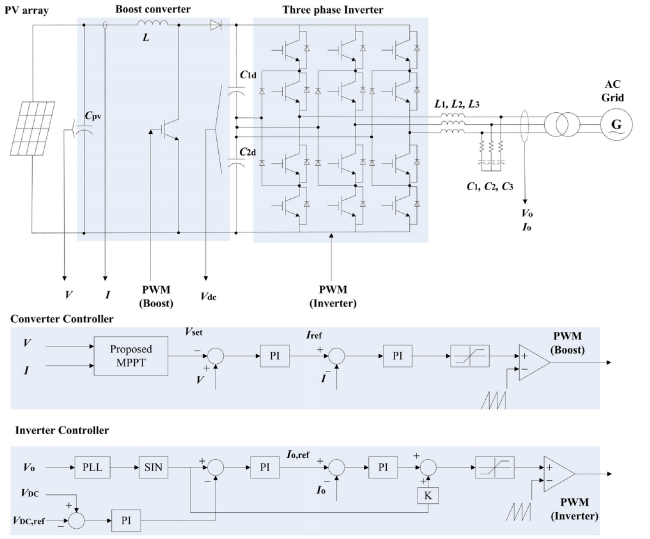

Fig. 6 *PV system structure diagram of a DC/DC + DC/AC two-stage grid-connected system*

Table 1 PV array parameters of the simulation model

Parameter	Symbol	Value
parallel configuration	N_p	41
series configuration	N_s	8
open-circuit voltage of each PV module	$V_{oc,md}$	64.2 V
short-circuit current of each PV module	$I_{sc,md}$	5.96 A
MPP Voltage of each PV module	$V_{mp,md}$	54.7 V
MPP current of each PV module	$I_{mp,md}$	5.58 A

PV power. If the PV power and voltage varies higher than a predetermined value, the PS detection process is activated.

To detect the PS, two criteria are applied to improve the accuracy of the detection. If one of the following criteria is satisfied, a PS is conformed, and the global search process starts to work.

$$\left|\Delta V\right| = \left|V_{pv} - V_{mpc}\right| > \Delta V_{SET} \tag{12}$$

$$n_w < N_{ser} \tag{13}$$

where $\triangle V_{SET}$ is a predetermined voltage reference chosen according to the PV array output voltage.

2.4.2 Global search process: If a PS is confirmed, the scheme enters the global search process, and the voltage reference for the boost converter controller is set according to the following formula.

$$V_{set}(n_w) = n_w[1 + \beta_{oc}(T - 298)]\left(V_{mp,md,STC} + \frac{N_s nkT}{q}\ln\frac{I_{mp}}{I_{mp,STC}}\right) \tag{14}$$

where $V_{set}(n_w)$ is the voltage reference with n_w working modules in a series, n_w is set in order from N_{ser} to 1 or until at least one of the following conditions is satisfied.

$$V_{set}(n_w) < V_{min} \tag{15}$$

$$P > P_c(T, n_w - 1) \tag{16}$$

where V_{min} is the minimum voltage of the PV inverter, $P_c(T, n_w - 1)$ is the calculate PV array power under 1000 W/m^2 and T with $n_w - 1$ working modules in a series.

$P_c(T, n_w - 1)$ is defined as follows:

$$P_c(T, n_w - 1) = P_{mp,STC}[1 + \gamma(T - T_{STC})]\frac{n_w - 1}{N_{ser}} \tag{17}$$

To avoid a wrong global MPP, an IC method with variable step size is executed until a local MPP is found and a predetermined minimum time is met after each set of the voltage reference. As $V_{set}(n_w)$ is an approximation of $V_{mp}(n_w)$ and some multiple local maxima may have similar value, thus a wrong global MPP is easily obtained in these cases. After searching all $V_{set}(n_w)$ or until the stop criteria are met, the recorded GMPP V_{mp} is set to the converter, and the scheme is back to the local process.

2.4.3 Local search process: In (12), the array temperature is needed to acquire V_{mpc} as defined in (11). The array temperature can be obtained using temperature sensors or by the following calculation method in this process. The temperature calculation is implemented if (i) all bypass diodes are blocking, (ii) the inverter is working at steady state, (iii) and the PV current is above a predetermined level. The temperature is derived from the MPP power P_{mp} formula as follows:

$$T = \frac{PI_{mp,STC}}{\gamma_{mp}P_{mp,STC}I} - \frac{1}{\gamma_{mp}} + T_{STC} \tag{18}$$

where P is the PV array MPP power, $P_{mp,STC}$ is the MPP power under STC, $I_{mp,STC}$ is the PV array MPP current under STC, and γ_{mp} is the temperature coefficient of MPP power.

The local search process is used to trace the MPP precisely using a modified PI-IC method. If $|dP/dV| > K_2$, the duty cycle is set as:

$$D(k) = D(k - 1) + \Delta D(k) \tag{19}$$

where $D(k)$ is the kth iteration of duty cycle D, ΔD is step size of the duty cycle chosen according to the slope of the P–V curve. Small, medium and large step sizes are used in the local process.

If $|dP/dV| < K_2$, the duty cycle with a variable step size is set as follows:

$$D(k) = D(k - 1) + l\Delta D(k) \tag{20}$$

where l is a coefficient defined as follows:

$$l = \left|I + V\frac{dI}{dV}\right| \tag{21}$$

If the operating point is close to the MPP, then a more precise and robust adjustment of D is implemented to promote the tracking effectiveness and the stability. If $\Delta D(k)\Delta D(k - 1) < 0$, it means the operating point is close to the MPP, and the duty cycle is set as (19) and $\triangle D$ is set as follows:

$$\Delta D(k) = -\Delta D(k - 1)/2 \tag{22}$$

3 Results

As shown in Fig. 6, the proposed MPPT scheme is applied in a two-stage grid-connected PV system. The simulation model is built in Matlab/Simulink environment. The PV array parameters used in this simulation model are shown in Table 1 and the PV system structure diagram is shown in Fig. 6. The PV array is divided into four subassemblies. Each subassembly includes two modules in each string. The PV inverter adopted in this system is a two-stage PCS rated as 100 kW with a prototype consisted of a boost converter and a three-phase full-bridge inverter. The PV inverter parameters are shown in Table 2.

The methods are tested under two kinds of shadings and two temperatures conditions. On the one hand, one condition is set as step-changing insolation, and the other condition is set as gradual-changing insolation. On the other hand, the module temperature is

Table 2 Parameters of the two-stage PV PCS of the simulation model

Parameter	Symbol	Value
input voltage range	V_i	200–1000 V
DC-Link voltage	V_{dc}	750 V
output Voltage	V_o	400 V
output current rating	I_o	250 A
boost Converter switching frequency	f_c	5 kHz
inverter switching frequency	fi	2.5 kHz

Table 3 Step-changing insolation designed in the simulation experiment

Time, s	Insolation, W/m^2			
	Assembly 1	Assembly 2	Assembly 3	Assembly 4
0–0.3	1000	1000	1000	1000
0.3–0.7	1000	800	600	400
0.7–1	1000	800	200	400
1–1.2	1000	1000	1000	750
1.2–1.5	1000	1000	1000	1000
1.5–2	1000	1000	650	1000
2–2.3	1000	1000	1000	1000
2.3–2.5	800	800	800	800
2.5–2.75	600	600	400	400
2.75–3	600	600	300	400

Table 4 Gradual-changing insolation designed in the simulation experiment

Time, s	Insolation, W/m^2			
	Assembly 1	Assembly 2	Assembly 3	Assembly 4
0–0.3	1000	1000	1000	1000
0.3–1.5	1000	1000	1000	S_v[a]
1.5–3	1000	1000	1000	700

[a] $S_v = \frac{-400}{1.2}(t - 0.3) + 1000.$

Table 5 Simulation results of the step-changing insolation under steady state at 25°C

Time, s	PV array output power, kW		Efficiency, %
	Simulation values	MPPT results	
0–0.3	100.13	100.10	99.97
0.3–0.7	48.15	48.04	99.77
0.7–1	41.49	41.43	99.86
1–1.2	81.69	81.52	99.79
1.2–1.5	100.13	99.85	99.72
1.5–2	74.93	74.9	99.96
2–2.3	100.13	99.85	99.72
2.3–2.5	79.02	78.98	99.95
2.5–2.75	40.57	40.46	99.73
2.75–3	31.71	31.16	98.27

set as 25°C and 50°C. The insolation setting is shown in Tables 3 and 4. The results of the PV array output are depicted in Fig. 7.

In Table 3, the step-changing insolation includes uniform insolation and non-uniform insolation. The insolation is decided to simulate the PS occurring, shading change, shading vanishing, and uniform insolation variation. The output powers in the steady state under step-changing insolation are shown in Tables 5 and 6. The results show that the algorithm can track the GMPP accurately with steady-state efficiency more than 99.5% in most cases. At some severe partial shading condition such as $t = 2.75$–3 s, the efficiency may drop below 99%.

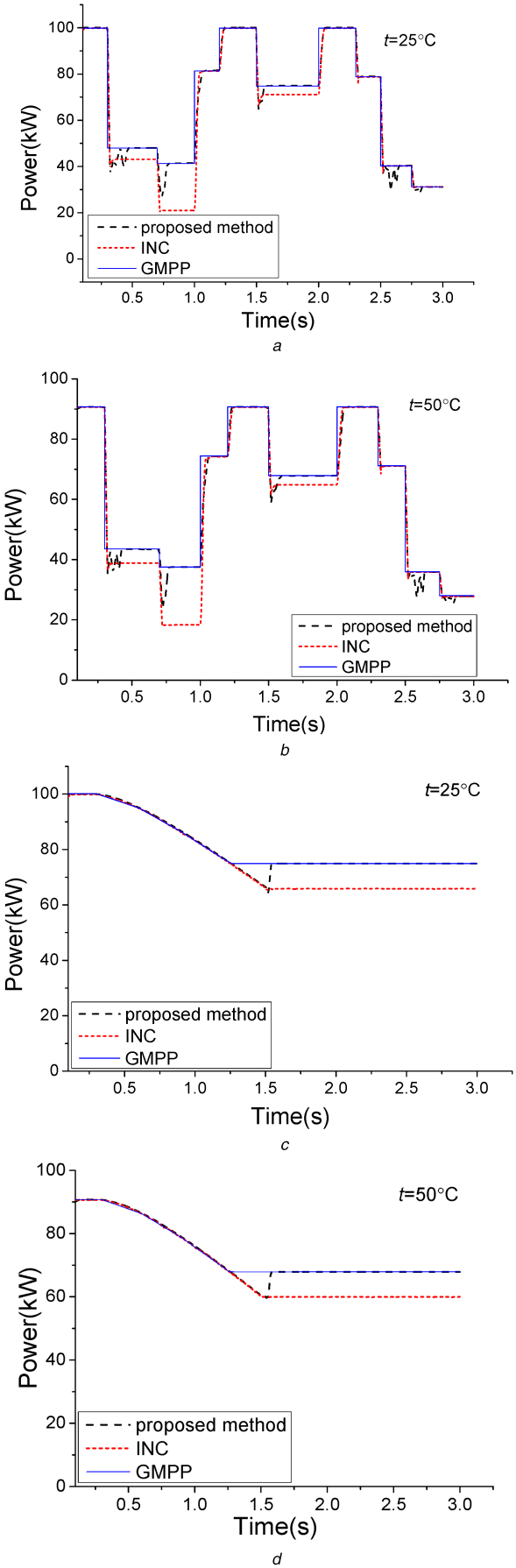

Fig. 7 *Simulation results of the proposed MPPT scheme and conventional IC methods*

(a) $t = 25$°C, step-changing insolation, ***(b)*** $t = 50$°C, step-changing insolation, ***(c)*** $t = 25$°C, gradual-changing insolation, ***(d)*** $t = 50$°C, gradual-changing insolation

Table 6 Simulation results of the step-changing insolation under steady state at 50°C

Time, s	PV array output power, kW		Efficiency, %
	Simulation values	MPPT results	
0–0.3	90.75	90.71	99.96
0.3–0.7	43.55	43.43	99.72
0.7–1	37.58	37.54	99.89
1–1.2	74.40	74.27	99.83
1.2–1.5	90.75	90.71	99.96
1.5–2	67.90	67.88	99.97
2–2.3	90.75	90.71	99.96
2.3–2.5	71.17	71.13	99.94
2.5–2.75	35.98	35.89	99.75
2.75–3	28.04	27.80	99.14

In addition, the behaviour of the proposed method is compared with the conventional IC algorithm. The results of the proposed and the compared MPPT algorithm are illustrated in Fig. 7. The results of the conventional IC method show that the operating point at steady state is usually the local maxima power point with the maximum voltage of the local maximas. It can only track the GMPP when no bypass diode blocked or under some serious PS such as at $t = 2.75$–3.0 s as shown in Figs. 7*a* and *b*.

As shown in Figs. 7*a* and *b*, the insolation was set to simulate one to four LMPPs to validate the effectiveness of the proposed scheme under different temperature and step-changing insolation. At $t = 0.3$ s, the insolation dropped from 1000 W/m^2 and produced four local maximas. The GMPP was the second peak (counted from the right of the *I*–*V* curve). Under this condition, the global search process scanned three local maxima and returned the voltage of the second peak. At $t = 0.7$ s, when the insolation dropped, and the GMPP moved from the second peak to the third peak. The global process was triggered. It scanned three local maxima and returned the GMPP within 0.2 s. At $t = 1.0$ s, as the insolation rose, the number of LMPP dropped from four to two. The GMPP moved to the first peak. Then, the global process only scanned one LMPP and met termination criteria. At $t = 1.2$ s, the shading vanished, and the algorithm confirmed that the insolation was consistent and remained in the local process. Under other conditions, such as $t = 1.5$ s, $t = 2.5$ s and $t = 2.75$ s, these GMPPs were all obtained within 0.2 s. At $t = 2.3$ s, a consistent insolation reduction was performed, and it remained in the local process before and after the insolation changed. The global process was not triggered because the voltage variation was less than the pre-set voltage ΔV_{SET}.

As shown in Figs. 7*c* and *d*, when the insolation changed gradually, the initialisation process was not triggered because it had not entered the steady state. After the operating point arrived at a steady state, the initialisation process started, and the algorithm detected the PS condition. Global search process found the GMPP and entered a new steady state within 0.05 s. Both under 25°C and 50°C, the method could detect the PS and track the GMPP accurately and fast under this condition.

In the simulation experiments, ΔV_{SET} is a key element to detect the PS accurately. If ΔV_{SET} is set too small, it increases wrong triggers of the global search when the uniform insolation changes. If ΔV_{SET} is set too large, it reduces accurate trigger of the global search under PS. Therefore, the GMPP cannot be tracked accurately. The setting of ΔV_{SET} is predetermined by try and error method. Also, if the temperature effect of ΔV_{SET} is not considered in (15), the GMPP cannot be tracked in every case under 50°C. In the same way, if $V_{set} = 0.8 N_{ser} V_{oc}$ proposed in other literature is used, the MPPT scheme would fail if the temperature effect is not considered.

4 Conclusion

The PV system has the multiple maxima problem under PS condition which has a significant influence on the system productivity. To solve this problem, this paper focuses on the accurate detection of PS and proposes a modified IC MPPT scheme. The PS is identified using the PV array information, PV power and voltage fluctuation and deviation. It demonstrates that the voltage of local maximum power point varies under the uniform insolation and PS when the system produces the same output current. Therefore, the voltage deviation can be used as the reference to detect PS. The PS detection is triggered when the operating point reaches a steady state after an insolation change occurs. Once the PS is confirmed, the MPPT scheme enters the global process. In the global process, an IC method with variable step size is employed. The exploring is finished until the stop criteria are met. Then, the MPPT scheme is back to the local process.

To validate the effectiveness of the proposed method, a two-stage grid-connected PV system integrated with the MPPT scheme is built in MATLAB/Simulink. The simulation results demonstrate the accuracy of PS detection and GMPP search under gradual-changing, step-changing insolation, and under different temperature. The search periods are about 0.1–0.2 s, and the efficiencies of generation under steady state are above 99.5% in most cases. The PS detection method can be applied in modified approaches and also the soft computing–based methods. The proposed MPPT scheme is expected to apply in BIPV where the PS is easily caused by surrounding environment as well as PV power plants where the unexpected PS has a severe influence on the PV generation.

5 Acknowledgments

The authors gratefully acknowledge the financial support from National Key Research and Development Program (2017YFB0903202), Guangzhou Innovation Platform and Sharing Project (201509010018) and Foshan Science and Technology Innovation Project (2016AG10011).

6 References

[1] Ishaque, K., Salam, Z.: 'A review of maximum power point tracking techniques of PV system for uniform insolation and partial shading condition', *Renew. Sust. Energy Rev.*, 2013, **19**, pp. 475–488

[2] Liu, L., Meng, X., Liu, C.: 'A review of maximum power point tracking methods of PV power system at uniform and partial shading', *Renew. Sust. Energy Rev.*, 2016, **53**, pp. 1500–1507

[3] Ishaque, K., Salam, Z., Taheri, H., *et al.* 'Modeling and simulation of photovoltaic (PV) system during partial shading based on a two-diode model', *Simul. Modelling Pract. Theory*, 2011, **19**, (7), pp. 1613–1626

[4] Esram, T., Chapman, P.L.: 'Comparison of photovoltaic array maximum power point tracking techniques', *IEEE Trans. Energy Convers.*, 2007, **22**, (2), pp. 439–449

[5] Femia, N., Petrone, G., Spagnuolo, G., *et al.*: 'Optimization of perturb and observe maximum power point tracking method', *IEEE Trans. Power Electron.*, 2005, **20**, (4), pp. 963–973

[6] Abdelsalam, A.K., Massoud, A.M., Ahmed, S., *et al.*: 'High-performance adaptive perturb and observe MPPT technique for photovoltaic-based microgrids', *IEEE Trans. Power Electron.*, 2011, **26**, (4), pp. 1010–1021

[7] Kuo, Y.-C., Liang, T.-J., Chen, J.-F.: 'Novel maximum-power-point-tracking controller for photovoltaic energy conversion system', *IEEE Trans. Ind. Electron.*, 2001, **48**, (3), pp. 594–601

[8] Liu, F., Duan, S., Liu, F., *et al.*: 'A variable step size INC MPPT method for PV systems', *IEEE Trans. Ind. Electron.*, 2008, **55**, (7), pp. 2622–2628

[9] Liu, Y.-H., Chen, J.-H., Huang, J.-W.: 'A review of maximum power point tracking techniques for use in partially shaded conditions', *Renew. Sust. Energy Rev.*, 2015, **41**, pp. 436–453

[10] Subudhi, B., Pradhan, R.: 'A comparative study on maximum power point tracking techniques for photovoltaic power systems', *IEEE Trans. Sustain. Energy*, 2013, **4**, (1), pp. 89–98

[11] Patel, H., Agarwal, V.: 'Maximum power point tracking scheme for PV systems operating under partially shaded conditions', *IEEE Trans. Ind. Electron.*, 2008, **55**, (4), pp. 1689–1698

[12] Renaudineau, H., Houari, A., Martin, J.P., *et al.*: 'A new approach in tracking maximum power under partially shaded conditions with consideration of converter losses', *Sol. Energy*, 2011, **85**, (11), pp. 2580–2588

[13] Azizi, K., Ghaffari, A.: 'Parameter estimation of photovoltaic panels and a model-based maximum power point tracking algorithm', *J. Renew. Sustain. Energy*, 2016, **8**, (4), p. 043504

[14] Zhu, X., Liu, S., Wang, Y.: 'A fast maximum power point tracking method for photovoltaic arrays under partially shaded conditions', *J. Renew. Sustain. Energy*, 2016, **8**, (2), p. 023504

[15] Karatepe, E., Hiyama, T., Boztepe, M., *et al.*: 'Voltage based power compensation system for photovoltaic generation system under partially

shaded insolation conditions', *Energy Convers. Manage.*, 2008, **49**, (8), pp. 2307–2316
[16] Syafaruddin Karatepe, E., Hiyama, T.: 'Performance enhancement of photovoltaic array through string and central based MPPT system under non-uniform irradiance conditions', *Energy Convers. Manage.*, 2012, **62**, pp. 131–140
[17] Shaiek, Y., Ben Smida, M., Sakly, A.*, et al.*: 'Comparison between conventional methods and GA approach for maximum power point tracking of shaded solar PV generators', *Sol. Energy*, 2013, **90**, pp. 107–122
[18] Miyatake, M., Veerachary, M., Toriumi, F.*, et al.*: 'Maximum power point tracking of multiple photovoltaic arrays: a PSO approach', *IEEE Trans. Aerosp. Electron. Syst.*, 2011, **47**, (1), pp. 367–380
[19] Fathy, A., Rezk, H.: 'A novel methodology for simulating maximum power point trackers using mine blast optimization and teaching learning based optimization algorithms for partially shaded photovoltaic system', *J. Renew. Sustain. Energy*, 2016, **8**, (2), p. 023503
[20] Liu, Y.-H., Huang, S.-C., Huang, J.-W.*, et al.*: 'A particle swarm optimization-based maximum power point tracking algorithm for PV systems operating under partially shaded conditions', *IEEE Trans. Energy Convers.*, 2012, **27**, (4), pp. 1027–1035
[21] Renaudineau, H., Donatantonio, F., Fontchastagner, J.*, et al.*: 'A PSO-based global MPPT technique for distributed PV power generation', *IEEE Trans. Ind. Electron.*, 2015, **62**, (2), pp. 1047–1058
[22] Seyedmahmoudian, M., Mekhilef, S., Rahmani, R.*, et al.*: 'Maximum power point tracking of partial shaded photovoltaic array using an evolutionary algorithm: a particle swarm optimization technique', *J. Renew. Sustain. Energy*, 2014, **6**, (2), p. 023102
[23] Xiao, W., Ozog, N., Dunford, W.G.: 'Topology study of photovoltaic interface for maximum power point tracking', *IEEE Trans. Ind. Electron.*, 2007, **54**, (3), pp. 1696–1704
[24] Walker, G.R., Sernia, P.C.: 'Cascaded DC–DC converter connection of photovoltaic modules', *IEEE Trans. Power Electron.*, 2004, **19**, (4), pp. 1130–1139
[25] Ahmed, N.A., Miyatake, M.: 'A novel maximum power point tracking for photovoltaic applications under partially shaded insolation conditions', *Electr. Power Syst. Res.*, 2008, **78**, (5), pp. 777–784
[26] Jiang, L.L., Maskell, D.L., Patra, J.C.: 'A novel ant colony optimization-based maximum power point tracking for photovoltaic systems under partially shaded conditions', *Energy Build.*, 2013, **58**, pp. 227–236
[27] Kouchaki, A., Iman-Eini, H., Asaei, B.: 'A new maximum power point tracking strategy for PV arrays under uniform and non-uniform insolation conditions', *Sol. Energy*, 2013, **91**, pp. 221–232
[28] Ji, Y.-H., Jung, D.-Y., Kim, J.-G.*, et al.*: 'A real maximum power point tracking method for mismatching compensation in PV array under partially shaded conditions', *IEEE Trans. Power Electron.*, 2011, **26**, (4), pp. 1001–1009
[29] Nguyen, T.L., Low, K.-S.: 'A global maximum power point tracking scheme employing direct search algorithm for photovoltaic systems', *IEEE Trans. Ind. Electron.*, 2010, **57**, (10), pp. 3456–3467